PRACTICAL CHARACTERIZATION OF CELL-ELECTRODE ELECTRICAL MODELS IN BIO-IMPEDANCE ASSAYS

Juan A. Serrano[1], Pablo Pérez[1], Andrés Maldonado[1], María Martín[2], Alberto Olmo[1], Paula Daza[2], Gloria Huertas[1] and Alberto Yúfera[1]

[1]*Instituto de Microelectrónica de Sevilla (IMSE), Universidad de Sevilla, Av Americo Vespuccio, S/N Sevilla, Spain*

[2] *Departamento de Biología Celular, Facultad de Biología, Universidad de Sevilla, Av. Reina Mercedes, S/N, Sevilla*

Keywords: Biomedical circuits; Impedance spectroscopy; Bioimpedance; Electrode-model; Oscillation Based Test circuits (OBT); ECIS.

Abstract: This paper presents the fitting process followed to adjust the parameters of the electrical model associated to a cell-electrode system in Electrical Cell-substrate Impedance Spectroscopy (ECIS) technique, to the experimental results from cell-culture assays. A new parameter matching procedure is proposed, under the basis of both, mismatching between electrodes and time-evolution observed in the system response, as consequence of electrode fabrication processes and electrochemical performance of electrode-solution interface, respectively. The obtained results agree with experimental performance, and enable the evaluation of the cell number in a culture, by using the electrical measurements observed at the oscillation parameters in the test circuits employed.

1 INTRODUCTION

Many research efforts have been devoted to find a reliable and robust non-invasive technique to estimate and study cell growth on a cell-culture assays (Khalil, 2014; Lu, 2009; Lei, 2014; Borkholder, 1998; Giaever, 1986) from several viewpoint. It can be found: toxicology assays (Daza, 2013), cancer characterization (Pradham, 2014; abdolahad, 2014) biochemical (Lourenco, 2016), immune-assays (Dibao-Dina, 2015), stem cells differentiation protocols (Reitingen, 2012), etc., that look to quantify the number of cells for characterizing a diversity of research objectives. Bioimpedance based (*BioZ*) measurements technique as ECIS, senses the electrical response generated on a biological sample, the cell-culture, when is excited with an AC electrical source, voltage or current, at several frequencies, as consequence of its conductivity properties. To obtain confident results, ECIS technique requires precise electronic circuits for picking-up the signals of interest (Grimmes, 2008), and accurate electrical models for the electrodes and cell-electrode-solution systems, mandatory for decoding the electrical measurements done by the circuits, and to express them in terms of cell number.

Several works on *BioZ* modelling and monitoring have been reported (Borkholder, 1998; Giaever, 1986; Huang, 2004), based on complex analytical approaches or Finite Element (FE) simulations of the whole cell-electrode-solution system. The obtained results are applied to mono-layer cell-culture configurations, fitting the proposed parameters and/or electrical circuits, to model the cell-electrode-solution. This article proposes a method to characterize an electric model for the cell-electrode interface in (Huang, 2004), using experimental data gathered from several experiments carried out in our research group. Our motivation is mainly derived from analysis of the parameter evolution observed on experiments, from the beginning of a cell growth assays, and before to win the confluent or mono-layer phase. These parameters associated to electrode models change from one electrode to

Serrano, J., Pérez, P., Maldonado, A., Martín, M., Olmo, A., Daza, P., Huertas, G. and Yúfera, A.
Practical Characterization of Cell-Electrode Electrical Models in Bio-Impedance Assays.
DOI: 10.5220/0006712601000108
In *Proceedings of the 11th International Joint Conference on Biomedical Engineering Systems and Technologies (BIOSTEC 2018) - Volume 1: BIODEVICES*, pages 100-108
ISBN: 978-989-758-277-6

another, and also in time, as consequence of electrochemical processes in electrode-solution-cell interfaces. The Fig. 1 shows the oscillation frequencies measured with our technique (Huertas, 2015) for eight different cell cultures in a growth curve assay. Each curve shows the oscillation frequency measured as a function of the time. The number of cell in the culture increases in time, depending of the cycle division of the cell line. Cell-cultures are done with commercial electrodes (Applied Biophysics), for several number of initial cells seeded: W1, W3: 2500 cells, W4, W5: 5000 cells; W7, W8: 10000 cells. From these responses, it can be concluded that:

1) Equal or similar oscillation frequencies were expected at the beginning of the assays, because cell density is very low. However, a wide frequency dispersion can be observed at t = 0 h, for example.
2) It will be expected a constant frequency response in cultures with only medium (W2 and W6). However, frequency response decreases in time from 790 Hz to 760 Hz, after one week (W2 and W6).
3) Responses of cultures with the same initial cells (W8-W7, W4-W5, W1-W3) should lead us to similar oscillation frequencies also. This is no true: measured frequencies (see W4 and W5 seeded with 5000 cells, for example) at the same times, are quite different.
4) The frequency dynamic range of the resulting frequencies changes between cultures, both for the same initial and different number of cells.

This experimental performance observed it is also detected for the amplitude of the oscillations (Fig. 1b). In all cases, measures were done with the same circuit, so measuring mismatching was not due to difference on circuit implementation. Considering these data, the electrical model for electrode-cell-solution system seems to change from electrode sample-to-sample, and in time, for the same electrode sample. This make not possible to consider a "static" model for the parameter values of the electrical model defining the performance of this system, in the sense that these parameters (resistance and capacitance values linked) will change for each sample, and also progress in time. It is proposed in this paper, on that basis of experimental result analysed, a "dynamic" matching of these parameters, once each experiment is finished. It is true that this approach does not allow full prediction of growth curves, but it will be demonstrated that errors in measured parameters (frequency and amplitude of the oscillations) are reduced by the matching method proposed in the following.

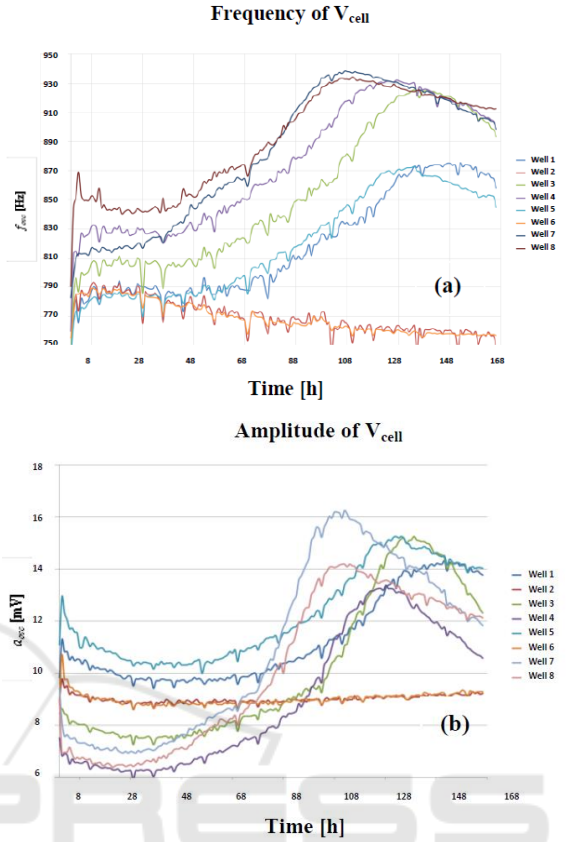

Figure 1: Measured time evolution of the oscillation frequency (a) and amplitude (b) of voltage signal Vcell. Curves corresponds to 2.500 cells (W1, W3), 5.000 cells (W4, W5) and 10.000 cells (W7, W8), seeded at t = 0, into separate well pairs. Wells W2 and W6 contain only medium.

The measurement system is described on section 2 with the sensing principle based on Oscillation Based Test (OBT) (Huertas, 2015). A method to solve the system equations is needed to obtain the oscillation amplitude (a_{osc}) and frequency (f_{osc}) (Huertas, 2015, Maldonado, 2016). Also, equations proposed to match experimental results are derived to put forward an electrical cell-electrode-solution model. Section 3 will describe the followed fitting process. Experimental results are described in section 4, and finally, conclusions are summarized in section 5.

2. MATERIALS AND METHODS

2.1 Cell-culture assay

Several experiments were carried out within one week. The electrodes employed for our tests are commercial electrodes from Applied Biophysics. These electrodes contain 8 separated wells with ten

circular biocompatible gold microelectrodes of 250 µm diameter. The biological sample under test is formed by Chinese hamster ovarian fibroblasts. This cell line is identified as AA8 (American Type Culture Collection). This sample is immersed in McCoy's medium supplemented with 10 % (v/v) foetal calf serum; 2mM L-glutamine, 50 µg/ml streptomycin and 50 U/ml penicilin. The growing environment is set at 37oC and 5% CO2 in a humid atmosphere. Different initial number of cells was planned for our experiments, either 2500, 5000 or 10000.

2.2 Cell-electrode electrical model

The biological sample under test is located on a two electrode system. The first one acts as a reference electrode and the second one is the measurement electrode. Cells are deployed on the electrodes alongside with medium solution. The electrical model describing this cell-electrode interface is presented on Fig 2a. This model has been explored on the literature in (Borkholder, 1998; Huang, 2004; Huertas, 2015). The sample is the connected to the oscillator as shown in Fig 2b, to build the biological sensor. A start-up signal is provided to the OBT to provide faster measurements and assure the optimal oscillation point for the system thus avoiding nonlinear behaviours of the electrical model. As it was mentioned in the previous section, the variation of the *BioZ* implies a change on the oscillator values, which is directly relate to the fill-factor, *ff*, on the cell culture, thus allowing us to measure cell population and growth.

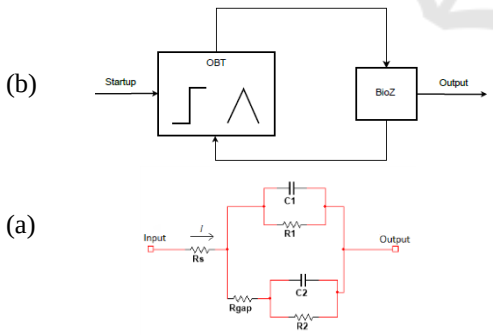

Figure 2. (a) Electric model of cell-electrode (*BioZ*). (b) Measuring circuit diagram.

The *BioZ* main electrical-model parameters are C, the double-layer capacitance arising from the cell electrode complex and *R*, the transfer resistance that represents biological sample resistance. Both elements are placed in parallel (Huang, 2004; Huertas, 2015). Fill-factor is presented as the cell covered area ratio in the electrodes (if there are not cells, is 0, and it is 1 when electrode is fully covered).

$$\begin{aligned} R_1 &= R/(1-ff) \\ C_1 &= C.(1-ff) \\ R_2 &= R/ff \\ C_2 &= C.f \end{aligned} \quad (1)$$

where C_1 and R_1 account for the empty microelectrodes contribution to the electrical response of the biological sample, and C_2 and R_2 depict the electrical response generated by the electrodes covered by cells. The R_s models the resistance which current must overtake to arrive at reference electrode. Finally, R_{gap} represents the resistance shaped at the gap or interface region between cell and electrode.

The model fitting process requires further knowledge on the circuit transfer function. Having analyzed the electrical model, next step is to define the transfer functions for the measuring system (Huertas, 2015; Maldonado 2016; Pérez, 2017). The analysis is presented below and summarized in eq. (2).

$$Z(s) = \frac{V(s)}{I(s)} = \frac{k_2 s^2 + k_1 \frac{\omega_o}{Q} s + k_0 {\omega_o}^2}{s^2 + \frac{\omega_o}{Q} s + {\omega_o}^2} \quad (2)$$

where,

$$k_2 = R_s \quad (3)$$

$$k_1 = R_s + \frac{R_{gap}.R_1}{2R_{gap} + R_1 + R_2} \quad (4)$$

$$k_0 = R_s + \frac{R_1(R_{gap} + R_2)}{R_{gap} + R_1 + R_2} \quad (5)$$

$$\omega_0 = \sqrt{\frac{R_{gap} + R_1 + R_2}{R_{gap}(RC)^2}} \quad (6)$$

$$Q = \omega_o . \frac{R_{gap} RC}{2R_{gap} + R_1 + R_2} \quad (7)$$

During the modelling adjustment process, three challenges were identified:

- Fill-factor: This is the measurement we aim to find out. This work is part of the process to obtain a reliable *ff* measurement out of the a_{osc} and f_{osc} acquired from the implemented sensor. To fit the model, we need to use a reliable reference for *ff* other than the measurements itself. This *ff* reference may be obtained from the microscopic analysis of the cell cultures under

test, but it can be the final solution because the ultimate goal is getting a sensing robust system to measure the number of cells without touch the cell-culture assay until the end of experiment.

- Non-constant value of the *BioZ* parameters along *ff*: The following Bode diagrams acquired from biological samples under test (Fig. 3) shows that magnitude at high frequencies can be used to determine R_s. However it is important to remark the differences among different days (cells are growing, hence increasing *ff*), which implies also variations on the R_s obtained values.

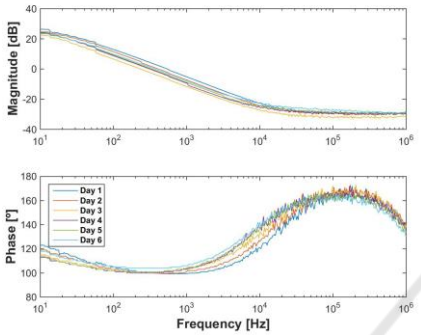

Figure 3: Bode diagram, magnitude and phase, for a single well during the experiment.

- Each well starts at different values of f_{osc} and a_{osc}: Fig. 4 illustrates small differences on each well in magnitude and phase during the experiment starting period. Experiment begins at several hundred Hertz, below 1 kHz, at this operation point each well has different frequency and amplitude values. The sample contains eight wells, each of them contain only either medium or cells with medium. These one start in an initial value of f_{osc} and a_{osc} which does not match with expected theoretical values for low *ff*. Experimental measurements tend to fit the expected values around 20 hours periods, corresponding to the cell division cycle.

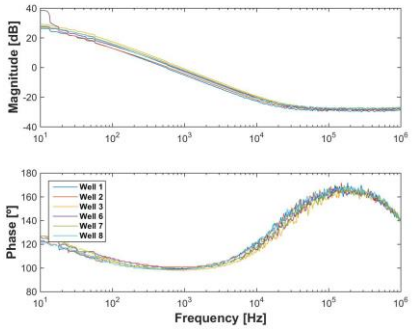

Figure 4: Bode diagram for each well on the first day.

2.3 Oscillator

Complete closed-loop system (circuit with *BioZ*) behaves like an oscillator (Fig 2 (b)). This is due to the circuit containing a non-linear element, a comparator in the feedback loop. Non-Linear system can present oscillations with a constant amplitude and frequency without external stimulation (limit-circles). According to describing-function method, non-linear component of the system can be linearized like it is presented in equation,

$$N(A,\omega) = \frac{Y}{X}\angle\phi \tag{8}$$

where N(A, ϕ) is an approximate linear form of the non-linear element, X is the sine input amplitude, Y is the amplitude of output fundamental harmonic component, and ϕ is phase difference of output fundamental harmonic component. In this case, describing function of comparator is shown in eq. (9).

$$N(A) = \frac{4V_{ref}}{\pi a_{osc}}.(-\cos(\theta_h) + \sin(\theta_h)) \tag{9}$$

where V_{ref} is the reference voltage for the comparator and θ_h is defined in eq. (10),

$$\theta_h = a\sin(\frac{h}{a_{osc}}) \tag{10}$$

being h the comparator hysteresis. The shape of describing-function has been defined. Additionally, the behaviour of the system is determined by the characteristic equation (11). If a solution exists for the given system, with a specific amplitude and frequency, means that the system is oscillating at that frequency with given amplitude.

$$1 + G(j\omega)N(A) = 0 \tag{11}$$

where G(jω) is the transfer function for the linear component of the system, which is the measurement circuit without the comparator and with *BioZ*. This is fulfilled when the following conditions are met:

1. A non-linear component must be part of the system. In this case non-linear part is the comparator.
2. Non-linear component does not depend on time.
3. Linear parts behave like a low-pass filter to guarantee that high frequency harmonics do not affect non-linear part. The system contains a band-pass filter, which avoid the input of non-fundamental harmonic components of the signal in the comparator.

4. Non-linearity is symmetrical, so there is not any DC component in the output signal when input signal is a sine.

With this method, theoretical a_{osc} and f_{osc} can be obtained depending on system parameters. Therefore, it is necessary to characterize a system model to compare theoretical and experimental results.

2.4 Sensitivity

To characterize an empirical model it is necessary to understand how changes in model parameters affect amplitude and frequency of the oscillation signal.

2.4.1 Fill-factor

It is important to understand the effects of *fill-factor* in the model of *BioZ*. Considering $ff \rightarrow 0$, we can conclude that $R_2 \rightarrow \infty$ and $C_2 \rightarrow 0$. Transfer function for *BioZ* is presented in eq. (12).

$$Z_{ff\rightarrow 0}(s) = (R \,\|\, C) + R_s \tag{11}$$

$$Z_{ff\rightarrow 0}(s) = \frac{R_s.(s + \frac{1}{(R_s \,\|\, R)C})}{s + \frac{1}{RC}} \tag{12}$$

where $Z_{ff\rightarrow 0}(s)$ is the impedance of cells for $ff \rightarrow 0$. Considering $ff \rightarrow 1$ we can conclude that $R_1 \rightarrow \infty$ and $C_1 \rightarrow 0$. Transfer function for *BioZ* is presented in eq. (14).

$$Z_{ff\rightarrow 1}(s) = (R \,\|\, C) + R_s + R_{gap} \tag{13}$$

$$Z_{ff\rightarrow 1}(s) = (R_s + R_{gap})\frac{(s + \frac{R + R_s + R_{gap}}{RC(R_s + R_{gap})})}{s + \frac{1}{RC}} \tag{14}$$

where $Z_{ff\rightarrow 1}(s)$ is the impedance of cells having $ff \rightarrow 1$.

From equations (13) and (14), the following statements are deduced. Low *ff* (experiment beginning) implies that R_{gap} does not affect model behavior. However, high *ff* implies greater effect on system model.

2.4.2 Poles and zeros location

It is necessary to identify the position of pole and zero in transfer function in eq. (14). These are defined on eq. (15) and eq. (16).

$$f_z(ff \rightarrow 0) = \frac{1}{2\pi C(R \,|\, R_s)} \approx \frac{1}{2\pi C R_s} \tag{15}$$

$$f_p(ff \rightarrow 0) = \frac{1}{2\pi RC} \tag{16}$$

It is possible now to calculate R_s and R using eqs. (17) and (18),

$$\lim_{f\rightarrow 0}(Z_{ff\rightarrow 0})(s)) = R_s + R \tag{17}$$

$$\lim_{f\rightarrow \infty}(Z_{ff\rightarrow 1})(s)) = R_s \tag{18}$$

by knowing the Bode diagram of the real system when the experiment starts and finishes. This task has been performed in three different experiments.

Fig. 4 shows Bode diagrams for well number one during each day of the experiment. First approach was to try to fit the model using such Bode diagrams but it was very difficult to find a suitable fit, as it is illustrated on Fig. 5.

Firstly, the model of *BioZ* is far from perfect, so that it is not possible to get a Bode diagram of the model similar to experimental Bode diagram. Secondly, it is difficult to reproduce similar magnitude and phase at the same frequency in model and experiment. Thus, it is necessary to find another way to fit the model. However, it is important to remark that zero is approximately at 15 kHz in every well and considered *ff*. To prove the use of 15 kHz as the zero value it is compared to another experiment, this is shown in Fig. 6. This experiment was performed in one day. Different cells concentrations were put on all wells, in ascending order, from well one (medium) until well eight (upper cells concentrations). Objective of this experiment is to obtain the Bode diagram of the system for each cell concentration without medium degradation.

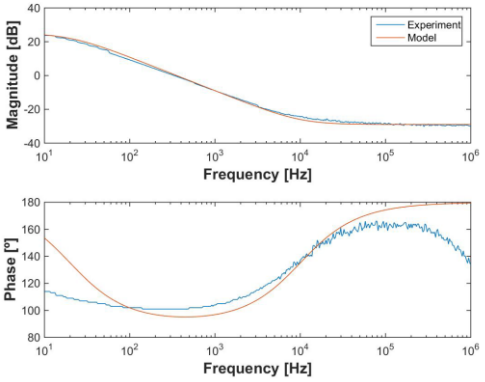

Figure 5: First approach fitting.

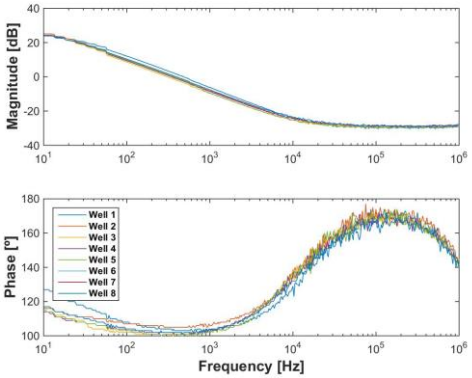

Figure 6: One day experiment

2.4.3: Other parameters

There are some parameters which are yet not characterized. It is important to consider the effect of these parameters in frequency and amplitude of the oscillator. Thank to electric simulator Multisim (and comparing with theoretical results of Matlab), the effects can be estimated using parametric sweeping. Some conclusions are provided below:

- *ff*→0 (beginning of the experiment):
  - Initial frequency can be selected only with position of the pole *fp*.
  - Initial amplitude can be selected using R_s and f_p. The R_s effect is significantly higher.
- *ff*→1 (end of the experiment). Frequency can be selected using R_{gap}, however it is important to remark that R_{gap} affect final amplitude as well.

It is possible to characterize the model parameters using this conclusions and eqs. (15) and (16).

2.5 Estimation of *ff*

During first experiment, which Bode diagrams were measured, wells were also photographed to estimate *ff* once a day until the end of the experiment. However, estimation of *ff* using photos was not accurate enough. On the following, a math temporal evolution estimation method for *ff* is presented.

Considering the area of the well is A_w=0.8 cm^2, approximate radio of cells is r_{cell} = 10 µm^2. Knowing the number of cells at the beginning of experiment as N_o and the division time of cells as t_r = 18 hours, it is possible to define a growth curve for (*ff*) in time.

$$N(k) = N_o 2^k \tag{19}$$

$$ff_k = \frac{N(k)\pi r^2_{cell}}{A_w} \tag{20}$$

Using eqs. (19) and (20), it is possible to calculate the number of cells and *ff* at a given moment, *k*, as is shown in Fig. 7.

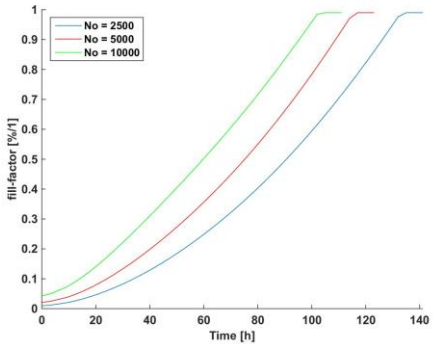

Figure 7: Estimated evolution of ff with No = 2.500, 5.000 and 10.000 cells.

3. Fitting model

There is enough information to fit the experiment model. Keeping in mind that f_z = 15 kHz, the algorithm to obtain the model:

Step 1: Select f_p using experiment initial frequency.

Step 2: Select R_s using experiment initial amplitude.

Step 3: Select R_{gap} using experiment final frequency.

Following this three steps, it is possible to fit a model which behaves similar to the experimental results. Even so, there is an amplitude error that increases with *ff*, observed in Fig. 8.

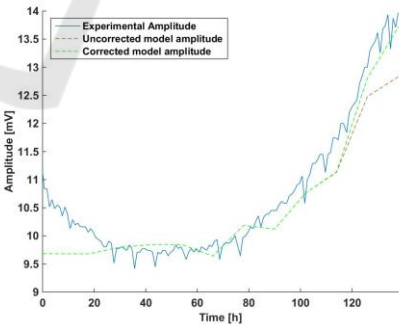

Figure 8: Comparison between experimental amplitude, uncorrected and corrected model amplitudes.

To solve this problem, first approach is to use the work presented in (Huang, 2004), but performing an alternative correction of R_s with *ff*. Moreover, it is decided that parameter R_s, which is calculated for *ff* →0, is an initial value of R_s, named R_{si}. R_s grows with *ff* during the whole experiment. R_s must match

the amplitude in $ff \rightarrow 1$. This is represented on eq. (21).

$$R_s(k) = R_{si} + \Delta R_s . ff(k)^n \quad (21)$$

where R_{si} is the initial value for R_s, ΔR_s is the range of R_s from $ff = 0$ to $ff = 1$, and n decided the growth rate of R_s until the maximum value (n=4 in this case). The eq. (21), represents R_s variation, allowing R_s to reach its final value when well is full ($R_s(ff \rightarrow 1) = R_{si}+\Delta R_s$). Finally, it is necessary to complete the fitting model selecting ΔR_s.

Step 4: Select ΔR_s using experiment final amplitude.

The Fig. 7 shows the effect of the evolution of R_s, with good agreement for amplitude estimation.

4. RESULTS

This section presents the results of the fitting method proposed before. Results are shown from Figures 9 to 11 (each figure shows one well with cells), and start from three different values of initial number of cells: 2500, 5000 and 10.000 cells. For each initial number of seeded cells, the time evolution of the *ff* is calculated according to eq. (20), and then, electrical simulations are performed in Multisim, considering the proposed parameters evaluated for the electrical model. The oscillation parameters, f_{osc} and a_{osc}, are measured and compared with the experimental ones.

In all cases, the amplitude and frequency errors are reduced, being possible to make the cell number estimation, at every time of the experiment. Errors observed at amplitudes are lower than frequencies. One of the main problems to fit the models of each well of the experiments is the small range of a_{osc} and f_{osc} found on the available data. Using this method, theoretical results are similar to experimental results.

5. CONCLUSIONS

It has been presented a fitting procedure to assign values to proposed parameters of the electrical-model in cell cultures assays. The proposal is useful in ECIS experiments to define the number of cells in a culture, giving a general solution, not only for cell monolayer configurations. For several initial values of cell seeded, results show that fitting models provide low error estimations for *ff* values. Thanks to *ff* estimation and R_S modification, it is possible to fit a model for each well knowing only a_{osc} y f_{osc} values at beginning and end of the experiment. A Matlab script has been developed to do this work automatically when experiment ends, either using theoretical equations of the system or using the software Multisim software to execute electrical simulations.

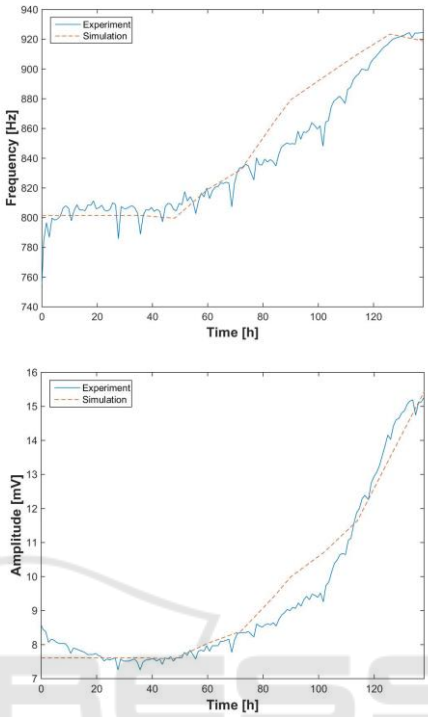

Figure 9: Comparison of frequencies and amplitudes between model and experiment for No = 2500 cells.

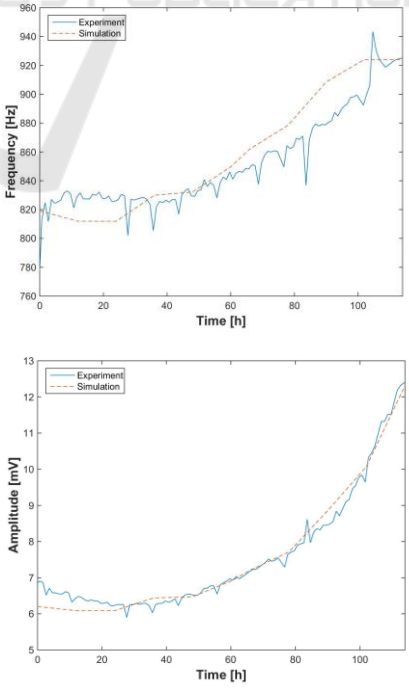

Figure 10: Comparison of frequencies and amplitudes between model and experiment for N_o = 5.000 cells.

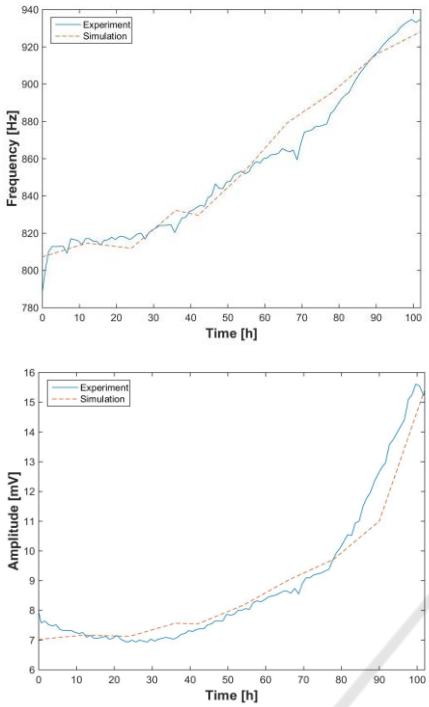

Figure 11: Comparison of frequencies between model and experiment for N_o = 10.000 cells.

ACKNOWLEDGMENT

This work was supported in part by the Spanish founded Project: Integrated Microsystems for cell culture test (TEC2013-46242-C3-1-P), co-financed with FEDER program.

REFERENCES

Abdolahad, M., Shashaani, H., Janmaleki, M., Mohajerzadeh, S., 2014. “Silicon nano grass based impedance biosensor for label free detection of rare metastatic cells among primary cancerous colon cells, suitable for more accurate cancer staging,”. Biosensors and Bioelectronics, 59, 151-159.

Applied Biophysics (http://www.biophysics.com/).

Borkholder, D. A., 1998. ”Cell based biosensors using microelectrode”. Ph D. Thesis.

Daza, P., Olmo, A., Cañete, D., Yúfera, A., 2013. “Monitoring living cell assays with bio-impedance sensors”. Sensors and Actuators B: Chemical. 176, 605-610.

Dibao-Dina, A., Follet, J., Ibrahim. M., Vlandas, A., Senez, V., 2015.“Electrical impedances sensor for quantitative monitoring of infection processes on HCT-8 cells by the water borne parasite Cryptosporidium,” at Biosensors and Bioelectronics, 66, 69-76.

Grimnes, S. and Martinsen, O., 2008. Bio-impedance and Bioelectricity Basics. 2nd edition. Academic Press, Elsevier.

Giaever, I. and Keese, C. R., 1986. “Use of Electric Fields to Monitor the Dynamical Aspect of Cell Behaviour in Tissue Cultures”. IEEE Transactions on Biomedical Engineering, vol. BME-33, nº 2, 242-247.

Huang, X., Nguyen, D., Greve, D. W. And Domach, M. M., 2004. ”Simulation of Microelectrode Impedance Changes Due to Cell Growth” IEEE Sensors Journal, vol. 4, nº. 5.

Huertas, G., Maldonado-Jacobi, A., Yúfera, A., Rueda, Huertas, J- L., 2015. “The Bio-Oscillator: A Circuit for Cell-Culture Assays,” IEEE Trans on CAS-II. 62, 164-168.

Khalil, S. F., Mohktar, M. S. and Ibrahim, F., 2014. ”The Theory and Fundamentals of Bioimpedance Analysis in Clinical Status Monitoring and Diagnosis of Diseases” Sensors, 14(6): 10895 – 10928.

Lei, K. F., 2014. ”Review on Impedance Detection of Cellular Responses in Micro/Nano Environment” Micromachines.

Lourenco, F., Ledoa, C. A., Laranjinhaa, J., Gerhardtc, G. A., Barbosa, R. M., 2016. “Microelectrode array biosensor for high-resolution measurements of extracellular glucose in the brain,”. Sensors and Actuators B: Chemical. 237, 298-307.

Lu, Y-Y., Huang, J-J. and Cheng, K-S., 2009. ”The design of electrode-array for monitoring the cellular bioimpedance” Industrial Electronics and Applications.

Maldonado, A., Huertas, G., Rueda, A., Huertas, J. L., Pérez, P. and Yúfera, A., 2016. ”Cell-culture measurements using voltage oscillations” IEEE 7th Latin American Symposium on CAS (LASCAS).

Pérez, P., Maldonado-Jacobi, A., López, A., Martínez, C., Olmo, A., Huertas, G. and Yúfera, A., 2017. “Remote Sensing of Cell Culture Assays. Cell Culture,” Chap 4: New Insights in Cell Culture Technology. 135-155. InTech Europe.

Pradham, R., Mandal, M., Mitra, A., Das, S., 2014. “Monitoring cellular activities of cancer cells using impedance sensing devices”. Sensors and Actuator B: Chemical, 193, 478-483.

Reitinger, S., Wissenwasser. J., Kapferera, W., Heer, R., Lepperdinger, G., 2012. “Electric impedance sensing in cell substrates for rapid and selective multipotential differentiation capacity monitoring of human mesenchymal stem cells,”. Biosensors and Bioelectronics, 34, 63-69.